

Ameriflux Working Document

Boundary Layer Group
College of Oceanic and Atmospheric Sciences
Oregon State University
Corvallis, OR 97331 USA

December 22 2004

1 Introduction

The goal is construct a quantitative and representative annual estimate for net ecosystem exchange of carbon (NEE) and to partition NEE into GEP (photosynthesis) and respiration components. However, there are numerous potential problems. Long periods of missing data that coincide with a particular stage of biological activity could contribute to bias in the annual estimate. The flux instruments have quality problems in wet weather, which includes most of the winter season in the study area. The open-path LICOR is subject to calibration drift as the condition of the surface of the windows changes. The flux measurement height may be in the roughness sublayer, especially in convective conditions, and there is no information on the horizontal or vertical variation of the flux. The single storage measurement site could be unrepresentative of the are due to preferred locations of nocturnal carbon dioxide accumulation. There could be a significant mismatch between the flux footprint and the storage footprint, especially in stable conditions. The fetch changes with wind direction and stability, and the wind direction and stability vary systematically with season and time of day. Advection may be significant, but is not known.

This document describes the methods used to arrive at annual NEE, GEP and respiration estimates.

2 Data collection

Fast response wind and temperature data from a sonic anemometer (Campbell CSAT3) and fast response number density data from a colocated open-path CO₂/H₂O analyser (LICOR-7500) are logged and saved at 20 hz for subsequent analysis. The mean CO₂ concentration profile is measured at multiple levels using a single closed-path gas analyser with multiple switching ports. Ancillary data can include mean temperature and wind profiles, radiation terms and soil properties.

3 Quality control

A complete description of this program is at

http://blg.oce.orst.edu/Software/QC_v3/guide/guide.html.

The qc program is applied to raw time series of fast response variables used in eddy correlation flux calculations. This variable set includes $(u, v, w, T_v, q, co2)$.

The program performs the following steps:

- Fast response specific humidity (gg^{-1}) and co2 concentration (ppm) are computed from fast response number density ($milli - molm^{-3}$) measurements and fast response ambient air density (temperature and pressure fluctuations). This is sometimes called a point-by-point WPL “correction”.
- Small segments of missing data in time series are replaced using linear interpolation. Small is defined as small enough such that the flux is not significantly effected, based on previous experience with other data sets.
- The times series are despiked. The spike threshold is 3.25 times the local standard deviation. Continious spikes for periods longer than 5 seconds are considered real events and not spikes. Spikes are replaced using linear interpolation. Some data that is flagged by the qc testing is subjected to a “heavy-despiking” algorithm that removes longer sequences of spikes.
- A series of tests are imposed that check the variable set for an unphysical range of values, unusally small or large variance, skewness and kurtosis, and for discontinuities in the mean. When suspect data is found it is masked out (set to missing data value).
- A fast response “clean” data set is written for subsequent analysis.

The LICOR-7500 has data quality problems when moisture (rain,snow,dew) gets on the windows. The CSAT generally has less problems than the LICOR-7500.

The quality control process is not 100% reliable. It is sometimes difficult to distinguish between instrument problems and rare but plausible physical behaviour.

4 Second generation

A complete description of this program is at

http://blg.oce.orst.edu/Software/2nd_and_3rdgen/.

This program computes means, variances, fluxes and spectra. Fluxes are computed for 3 different local averaging time scales; 100 seconds, 300 seconds and 600 seconds. For Ameriflux we use the 600-second fluxes. There is no detrending and fluxes are calculated using unweighted, non-overlapping, box-car averages. Fluctuations (e.g. w') for all points in the first 600-second window are computed by subtracting the 600-second mean. The same is done for co_2 . The product (e.g. $w'co_2'$) is then computed for all points in the window and then averaged over the window. This is repeated for the next 600-second window, etc.

No corrections are made for potential high frequency flux loss due to path-length averaging by the sonic or the LICOR, or for potential high frequency flux loss due to physical separation between the sonic and the LICOR.

Multiresolution cospectra and spectra are computed and saved for analysis of the scale-dependence of the fluxes.

We note that use of a 600-second local averaging time scale for computing fluxes in strongly stratified conditions may include poorly sampled mesoscale motions. As a result, the flux is characterized by large random sampling error. The contribution to the calculated flux at these large time scales (low frequencies) may be larger than the contribution from turbulent scales in very weak turbulence.

4.1 Tilt correction

A tilt correction is applied to the wind components prior to computing fluxes. The tilt correction can be time-dependent to accommodate changes in the sonic orientation due to any realignments that take place during the year. In this case, the entire procedure (see below) is repeated separately for each period. Individual hours with weak horizontal winds (less than 2 m s^{-1}) are excluded from the tilt correction development procedures since the tilt angle can be erratic in weak winds.

A practice constant offset is removed from the vertical motion making \bar{w} zero for the entire period. The removal of the offset does not directly affect the computed flux, since only a constant is removed for each record. However, we note that applying a subsequent tilt rotation to the data with no prior removal of the offset, converts the vertical motion offset into horizontal flow.

After removing the practice offset, a practice tilt angle is computed for each 1-hour record which eliminates the record mean vertical motion. These tilt angles are averaged over the entire period for a sequence of wind direction categories, giving wind direction-dependent average tilt angles. When the practice tilt angles appear to be consistent with a tilted anemometer, the actual tilt correction is applied. For each 1-hour data record, a lookup table is used to determine the offset and tilt angle to use depending on the time and the wind direction, and the rotation is done on the fast response wind components. The process includes a horizontal rotation to along-wind (u) and cross-wind (v) components such that $\bar{u} > 0$ and $\bar{v} = 0$ to distinguish between along- and cross-wind components of the wind stress. This method does not force the record-mean vertical motion to zero. The correction is applied to all records regardless of wind speed.

5 Third generation

A complete description of this program is at

http://blg.oce.orst.edu/Software/2nd_and_3rdgen/.

This program calculates quantities related to evaluating Monin Obukov similarity theory. Several estimates for different types of flux sampling errors are computed including random sampling error, systematic error, a flux intermittency parameter and flux non-stationarity.

Half-hour mean quantities are computed from the 2nd generation 600-second data. Three 10-minute average values are averaged to make one 30-minute average. A heat flux is calculated from the sonic heat flux (which is close to the virtual temperature flux) and the moisture flux.

6 Ameriflux processing

6.1 Flow distortion

The fluxes for half-hourly periods where the flow is potentially disturbed due to sonic support structures, other instruments or the tower itself are masked out (set to missing data value). The width of the wind sector deemed to have potential flow distortion is specific to each site and depends on the type of tower and the boom length.

6.2 Outliers

Flux outliers are removed to avoid their influence on gap-filling. Values of the eddy correlation (EC) flux outside a user specified range are masked out. The range is selected after consulting a time series plot of all the fluxes, and should include only a very small fraction of the data. It is likely that some of these outliers are associated with instrument problems that were not detected by the quality control testing.

6.3 Gap-filling

The steps in the gap-filling procedure are outlined below.

- 1. Temporal fill wide gaps using linear interpolation. A wide gap is a sequence of consecutive days with a very high percentage of missing

data (90% or more). Typically, the percent of missing data in these cases is 100%. When equivalent width data segments just prior to and subsequent to the wide gap segment have a lower percent missing data (60% or less), then linear interpolation is used to fill across the wide gap. Means are computed for the prior and subsequent segments for each of 48 half-hour periods. The half-hourly values are then interpolated across the wide gap. This procedure is implemented using a sequence of block windows of width 35,30,...10,5 days.

- 2. Vertical fill 1-pt and 2-pt gaps using linear interpolation for $co_2(z)$ and $T(z)$. A 1-pt gap is one vertical level with missing data with good data both above and below, for the same time period.
- 3. Temporal fill 1-pt and 2-pt gaps using linear interpolation for all variables. A 1-pt gap here is one half-hour with missing data with good data for the prior and subsequent half-hour periods.
- 4. The mean diurnal averages are calculated for all variables using all non-missing data within a 15 day window width. The mean diurnal average consists of the averages over the window for each of 48 half-hour periods during the day. Missing data within the window is replaced with the corresponding average over the window if at least 50% of the data for that period were included in the average. For example, if a particular half-hour period is missing for 8 or more of the 15 days in the window, the missing data for that half-hour period will not be replaced by the average.

This entire process is then repeated partitioning the data into 8 three-hour periods instead of 48 half-hour periods. The probability of finding enough data to meet the 50% criteria is greatly increased because the time-of-day criteria is relaxed from a half-hour to three-hours. In general, this will depend on the character of the missing data and could be site-specific. When replacing missing data with the average, the six half-hour averages in the three-hour period are all assigned the same

value.

- 5. Repeat step 4 for increasing window sizes of 30, 45, etc. days until all data is gap-filled for all variables.

6.4 Storage term

The storage of *co2* and heat between the ground and the flux measurement height is computed by vertically integrating the local time tendency. The time change is computed using centered ($2 \delta t$) differences and half-hour means. The vertical integration is done assuming a piecewise linear fit to the $co2(z)$ and $T(z)$ profile data. The profiles are extrapolated from the first measurement level down to the surface using the slope between the first and second levels.

6.5 u_* -filtering

Nocturnal measurements of the *co2* EC flux plus storage sometimes increase with increasing friction velocity (u_*). Since respiration is not thought to be function of u_* , this indicates that other processes may be acting. One interpretation is that horizontal or vertical advection of *co2* must be important. Another interpretation is that the storage measurement is unrepresentative, possibly due to horizontal heterogeneity of the storage. Another is that the flux footprint region could be quite different than the footprint of the storage measurement in stable flows.

One approach to this problem is to apply u_* filtering. A model of respiration is developed using the nocturnal $F_c + S_c$ measurements in only high u_* conditions, where high is defined as larger than a critical value. In these high mixing conditions, advection and horizontal heterogeneity are thought to be less important.

The friction velocity is calculated as the square root of the magnitude of the 30-minute averaged wind stress components

$$u_* = (\overline{w'u'^2} + \overline{w'v'^2})^{1/4}. \quad (1)$$

The critical u_* value is estimated in off-line mode by examining the u_* -dependence of $F_c + S_c$ in high u_* nocturnal conditions. The year can be broken up into a sequence of 60-day periods with a separate critical u_* for each period, if necessary.

Plots of nocturnal $F_c + S_c$ bin-averaged by u_* category are examined to see if and where a levelling off occurs with increasing u_* . Ideally, $F_c + S_c$ should not be sensitive to u_* for u_* larger than the critical value. We define “nocturnal” as the half-hour periods where the solar zenith angle exceeds ninety degrees.

Sensitivity tests indicate that the $F_c + S_c$ vs (u_*) relationship is heavily influenced by outliers. A more robust relationship is found after discarding points in the upper 2% and lower 2% of the frequency distribution of both $F_c + S_c$ and u_* . Negative nocturnal values of $F_c + S_c$ are discarded since such values are suspect probably due to large random flux sampling errors.

Once the critical u_* is determined, nocturnal $F_c + S_c$ for high u_* conditions is related to predictors of respiration, such as subcanopy air temperature, soil temperature and soil moisture. A model of respiration is developed. The precise form of the model depends on the special characteristics of the site and the availability of measurements. When available, soil chamber measurements of respiration are consulted in the model development.

6.6 Respiration, GEP and NEE

Respiration is estimated by applying the site specific model discussed above to all daytime and nocturnal periods regardless of mixing strength. Recall that the model coefficients were derived using the $F_c + S_c$ measurements for only the high u_* nocturnal periods, and can be specified separately for each 60-day period.

GEP is calculated as $F_c + S_c$ minus the modelled respiration during the day, and is set to zero at night. NEE is then given by GEP + respiration.

Respiration, GEP and NEE are defined as negative for carbon uptake by the ecosystem and positive for release of carbon to the atmosphere.

6.7 Annual NEE

Annual NEE (gCm^{-2}) is computed as

$$NEE = N_d \cdot 86400 \cdot 10^{-3} \cdot (12/44) \cdot A \quad (2)$$

where A is the annual average NEE ($mg\ co2\ m^{-2}s^{-1}$) and N_d is the number of days per year. The same approach is used for computing annual sums of respiration and GEP.

7 Application to IP03

The first application of the OSU-BLG processing was for the 2003 data from the intermediate pine site near Sisters, OR, USA. The above canopy flux measurements were made 31 m above ground using a CSAT3 sonic anemometer and open-path LICOR-7500. The average height of the canopy was 17 m , so the flux instruments were approximately 14 m above canopy, or at 1.8 canopy heights. Significant solar radiation reaches the forest floor underneath the canopy in summer indicating a fairly sparse canopy. During summer nights, the subcanopy layer remains significantly stratified even with the highest above canopy u_* conditions.

Mean $co2(z)$ (closed path LICOR-6262) was measured at 1, 4 and 30 m . Mean temperature (HOBOS) was measured at 3, 6, 10, 20 and 30 m . Mean horizontal winds (Handars) were measured at 3, 6, 10, 20 and 30 m . The soil heat flux was measured at 5 locations and averaged. Soil temperature was measured at 6 depths between 2 and 64 cm at one location. Soil moisture content was measured at one location. Automated daily mean chamber measurements of soil respiration were made during April through Spetember.

7.1 Data coverage

A total of 6790 hours of data were logged (78% annual coverage). Approximately 10% of these hours contained enough missing data that they could not be saved and were discarded. Approximately 10% of the surviving hours were discarded by quality control tests. Problems with either the *co2* or *h2o* measurement (usually both) from the LICOR-7500 were 25 times more likely to occur than problems with the CSAT.

Subsequent to quality control, a problem with the 31-m fluxes was discovered for the period 11-Sep to 29-Sep (DOY 255-272), and these data were discarded. An additional problem with the 31-m fluxes was discovered during the tilt correction phase of the processing for the period from 4-Nov to the end of the year, and these data were discarded. Apparently, the mount holding the sonic anemometer to the boom came loose.

Time series plots indicated that the gap-filling approaches did not work very well for heat fluxes during November and December where there was almost no good quality flux data. A special patch was applied for this period where H and LE were replaced by a linear model based on the net radiation. The model coefficients were developed from the data during the remaining part of the year (Jan-Oct). The large amount of missing data severely tested the gap-filling procedures.

Table 1. Percent of available EC *co2* flux (F_c) and storage (S_c) data.

Month	J	F	M	A	M	J	J	A	S	O	N	D
F_c	38	68	40	46	21	74	91	81	31	76	5	0
S_c	88	100	98	99	90	33	72	0	83	56	54	42

7.2 Respiration modelling

Nocturnal $F_c + S_c$ increases with increasing u_* at this site during some periods of the year (Figure 1). Based on these data, we select a critical u_* value of 0.5 m s^{-1} for the purpose of applying the u_* -filtering, and apply this constant value for the entire year. The respiration from nocturnal EC flux plus storage measurements during high u_* periods agrees reasonably well with the automated chamber measurements (horizontal lines in Figure 1). The eddy correlation estimates of respiration are slightly higher than the chamber values presumably due to respiration from the foilage, which would not be captured by the chamber measurements.

The subcanopy air temperature, 2-cm soil temperature and 4-cm soil temperature were all reasonably good predictors of respiration (measured nocturnal $F_c + S_c$ in high u_* conditions). We choose the 4-cm soil temperature. The temperature-dependence was fit to the form

$$R_{es} = \alpha T^\beta \quad (3)$$

using least squares regression. The respiration was first bin-averaged by temperature category (circles in Figure 2) and then the regression was done on the bin-averaged data to obtain the coefficients, $\alpha = 0.037$ and $\beta = 0.560$ and the model (solid line Figure 2). The model coefficients change to 0.033 and 0.595, respectively, using a critical u_* of 0.7 m s^{-1} instead of 0.5.

7.3 Annual estimates

The estimate of annual NEE at this site is perhaps high compared to expectations for a semi-arid ponderosa pine site (Table 2). As a sensitivity test, increasing the u_* threshold from 0.5 to 0.7 $m s^{-1}$ slightly decreases the respiration, and thus increases the annual carbon uptake, contrary to expectations. The fact that increasing the critical u_* from 0.5 to 0.7 does not increase the measured co2 flux is not conclusive since: 1) the amount of data is small and 2) the footprint increases with wind speed.

As another sensitivity test, discarding the u_* -filter approach and using the automated chamber measurements for respiration, decreases the annual respiration and increases the annual carbon uptake (Table 3). In this calculation, the respiration model with critical $u_* = 0.5 m s^{-1}$ is used when the chamber data is missing. The chamber measurements are not extrapolated into the winter season.

The July mean diurnal cycle of the terms in Table 2 (top row) is shown in Figure 3, while the annual cycle of weekly-averages is in Figure 4. These fields are based on the standard calculation with u_* -filtering and a threshold value of 0.5 $m s^{-1}$.

Table 2. Annual estimates (gCm^{-2}) for two critical u_* (ms^{-1}) values.

Critical u_*	F_c	S_c	GEP	R_{es}	NEE
0.5	-578	0	-1299	936	-363
0.7	-578	0	-1285	905	-380

Table 3. Annual estimates (gCm^{-2}) based on the automated chamber measurements of respiration.

F_c	S_c	GEP	R_{es}	NEE
-578	0	-1218	826	-392

7.4 Discussion

An under-estimate of respiration would contribute to the large negative NEE indicating relatively large carbon uptake compared to expectations for this site. Comparisons with the automated chamber measurements are inconclusive (Figure 5). In June and July with the warmest soil temperatures, the chamber measurements of respiration exceed our modelled estimate, however, the chamber estimates are significantly lower than the model estimates in the early and late summer. It is not clear why the chamber measurements drop off so sharply in late July and early August, while the soil temperature and soil moisture are not changing rapidly.

A possible reason for the relatively large NEE estimate is that even with strong mixing above the canopy (high u_* conditions), the mixing underneath the canopy is still suppressed due to a surprisingly strong temperature stratification. The stratification decreases with increasing u_* above the canopy as expected, but does not go to zero. In summer, the stratified layer results from strong radiative cooling at the surface due to clear skies, dry soil and a sparse canopy. Because of the suppressed mixing in the subcanopy layer, the nocturnal flux measurements made above the canopy may under-estimate the respiration even under the strongest mixing conditions observed.

Another potential complication is that when the wind is from the south or southwest, it is coming from a region of smaller LAI. The IP03 site is in an area of local maximum LAI. At night, the surface footprint is larger (enormous with subcanopy stratification) and is expected to be smaller with daytime heating. Therefore, the daytime carbon uptake is dominated by the high LAI area in the vicinity of the tower, while the nighttime respiration is more strongly influenced by lower LAI regions more removed from the tower site.

7.5 List of variables

# Doy	fractional day of year
# Hour	fractional hour of day
# Fc	ec co2 flux (mg CO2/m ² /s) CSAT3/LI-7500
# Fc.flag	Fc flag: 0=gap-filled ec co2 flux, 1=measured
# Sc	co2 storage (mg CO2/m ² /s) LI-6262
# Sc.flag	Sc flag: 0=gap-filled co2 storage, 1=measured
# NEE	net ecosystem exchange (mg CO2/m ² /s)
# Res	total respiration (mg CO2/m ² /s)
# GEP	gross ecosystem production (mg CO2/m ² /s)
# CO2	mean co2 concentration (mg CO2/m ³) from LICOR-6262
# LE	latent heat flux (W/m ²)
# H	sensible heat flux (W/m ²)
# Sh	heat storage term (W/m ²)
# Ustar	friction velocity (m/s)
# Rn	net radiation (W/m ²)
# PAR	photosyn active rad (micro-mol/m ² /s)
# Rg	shortwave global rad (W/m ²)
# G	soil heat flux (W/m ²)
# T	air temperature (C) from T/RH Vaisla
# RH	relative humidity from T/RH Vaisla
# WS	wind speed (m/s) from CSAT3
# WD	wind direction (degs) from CSAT3
# PREC	precipitation (mm)
# PRESS	barometric pressure (mb)
# Ts.2cm	soil temperature (C)
# Ts.4cm	soil temperature (C)
# Ts.8cm	soil temperature (C)
# Ts.16cm	soil temperature (C)
# Ts.32cm	soil temperature (C)

# Ts.64cm	soil temperature (C)
# SWC	soil water content (m ³ /m ³)
# Zenith	solar zenith angle (degs)
# VPD	vapor pressure deficit (mb)

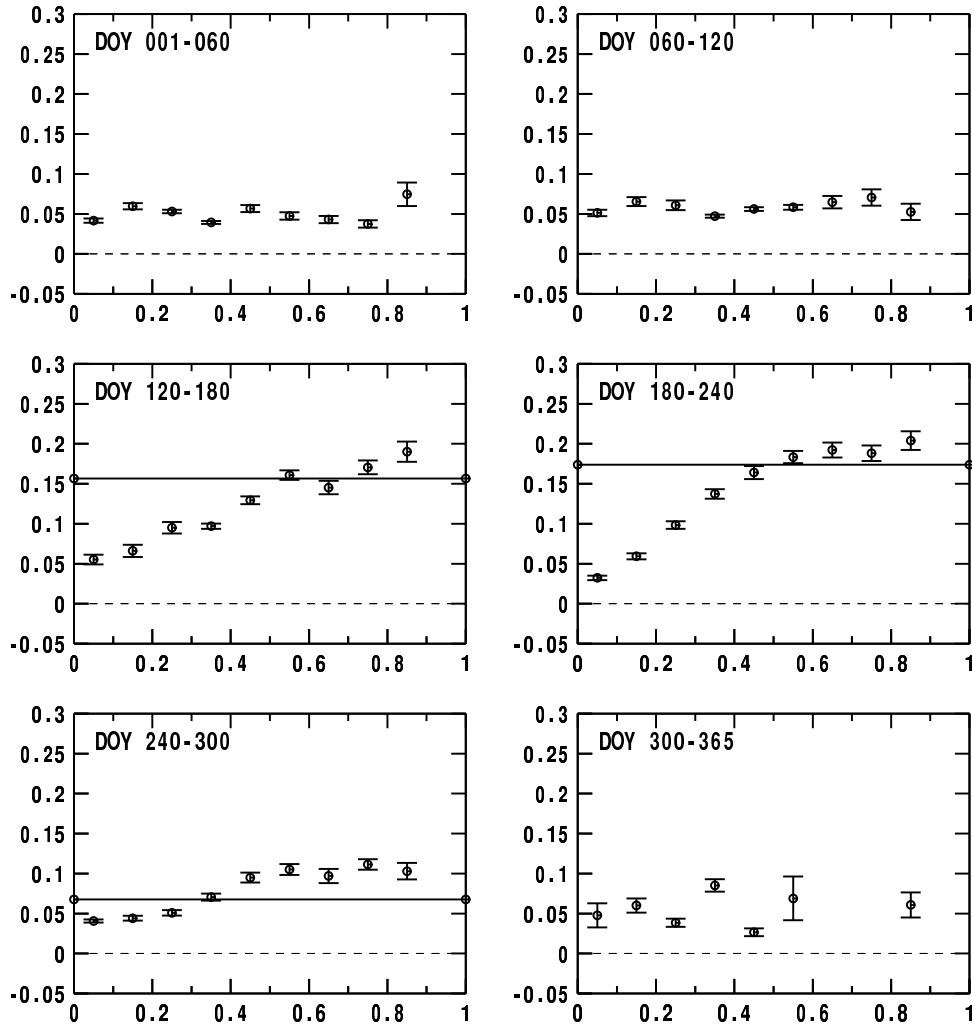


Figure 1: Seasonal pattern of bin-averaged nocturnal $F_c + S_c$ ($\text{mgm}^{-2}\text{s}^{-1}$) versus friction velocity (ms^{-1}) for IP03. Solid horizontal lines are estimates of daily mean soil CO_2 efflux (respiration) from automated chamber measurements, corrected using a relationship between manual and automated chamber data.

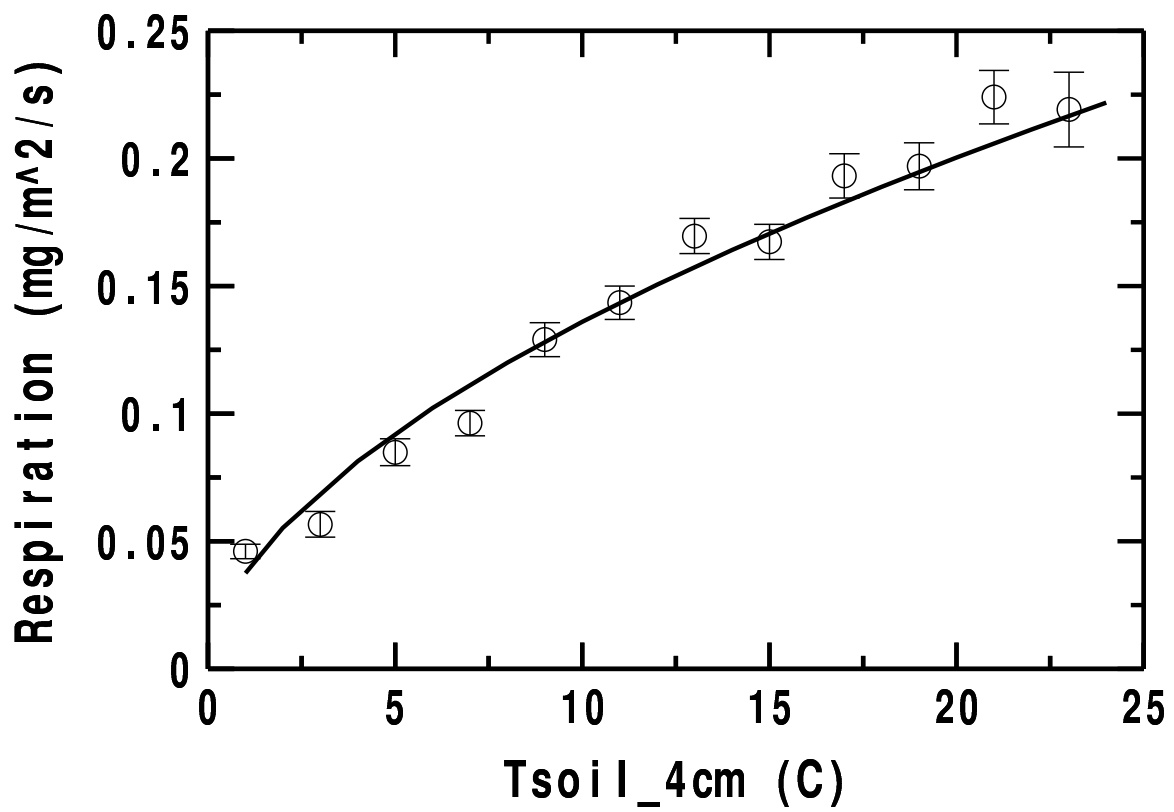


Figure 2: Temperature-dependent respiration model.

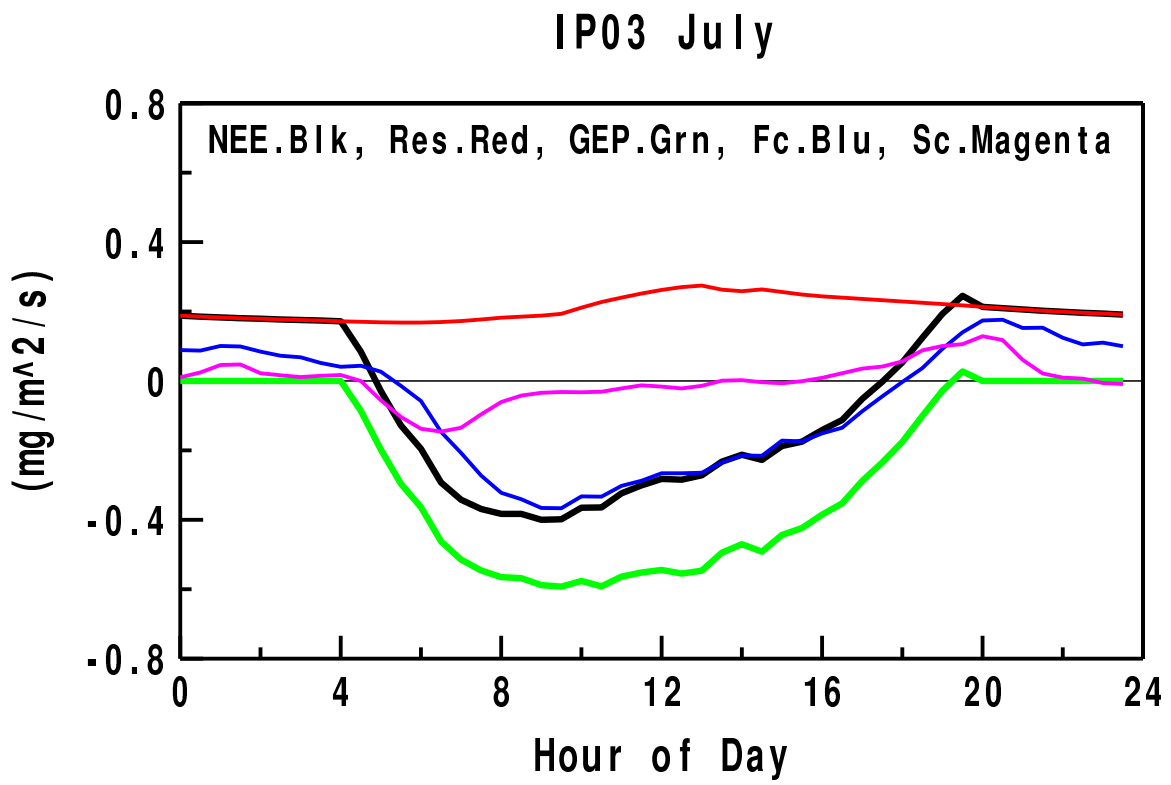


Figure 3: Average July diurnal cycle of selected quantities for IP03.

IP03 (weekly averages)

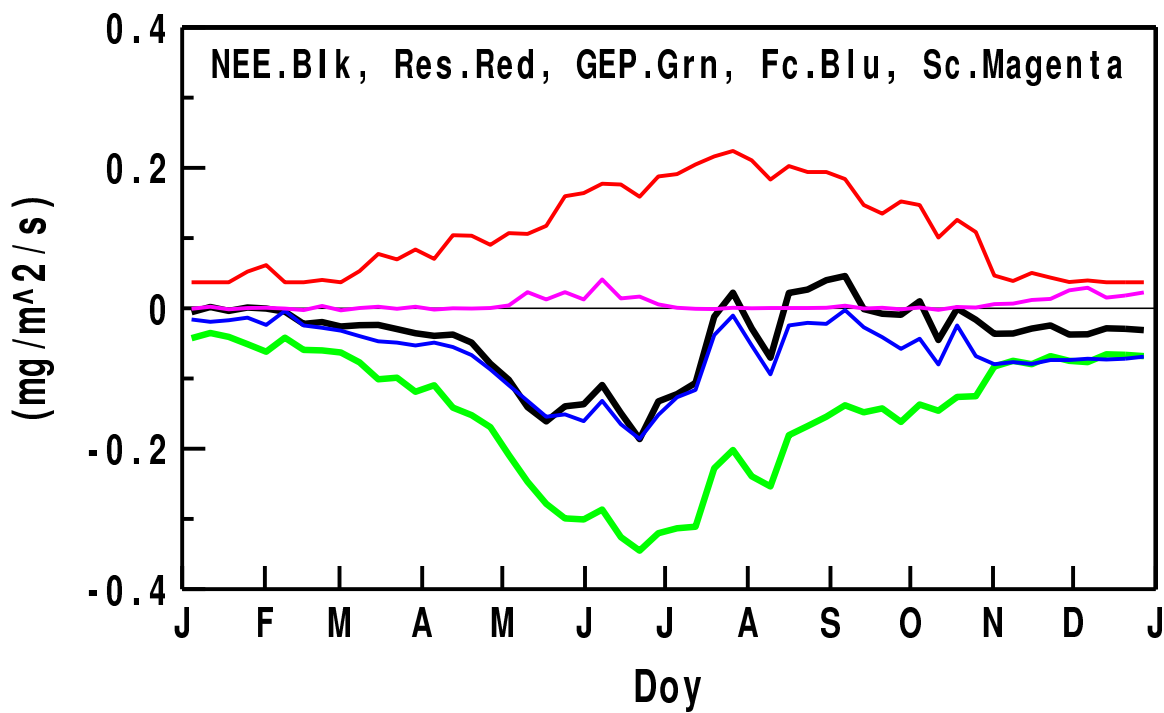


Figure 4: Annual cycle of weekly-averaged selected quantities for IP03.

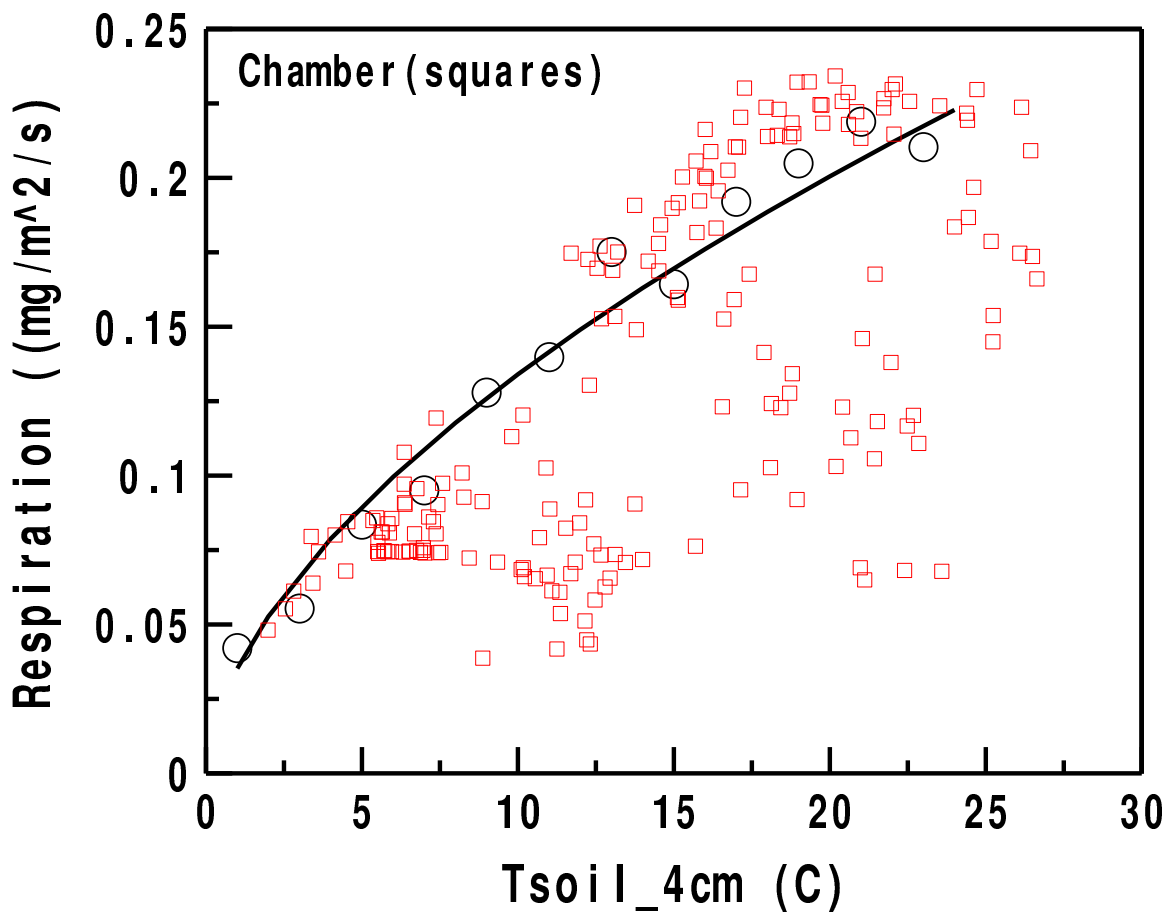


Figure 5: Temperature-dependent respiration model compared to the automated chamber measurements of respiration (red squares).